

Surface plasmon modulation induced by a direct-current electric field into gallium nitride thin film grown on Si(111) substrate

Amaud Stolz, Suk-Min Ko, Gilles Patriarche, Elhadj Dogheche, Yong-Hoon Cho et al.

Citation: *Appl. Phys. Lett.* **102**, 021905 (2013); doi: 10.1063/1.4776671

View online: <http://dx.doi.org/10.1063/1.4776671>

View Table of Contents: <http://apl.aip.org/resource/1/APPLAB/v102/i2>

Published by the [American Institute of Physics](#).

Related Articles

Highly localized heat generation by femtosecond laser induced plasmon excitation in Ag nanowires
Appl. Phys. Lett. **102**, 073107 (2013)

Observation of the electron-accumulation layer at the surface of InN by cross-sectional micro-Raman spectroscopy
Appl. Phys. Lett. **102**, 072101 (2013)

Toward surface plasmon polariton quantum-state tomography
J. Appl. Phys. **113**, 073102 (2013)

Sub-volt broadband hybrid plasmonic-vanadium dioxide switches
Appl. Phys. Lett. **102**, 061101 (2013)

Interaction of surface and interface plasmons in extremely thin Al films on Si(111)
Appl. Phys. Lett. **102**, 051605 (2013)

Additional information on *Appl. Phys. Lett.*

Journal Homepage: <http://apl.aip.org/>

Journal Information: http://apl.aip.org/about/about_the_journal

Top downloads: http://apl.aip.org/features/most_downloaded

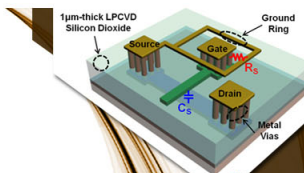
Information for Authors: <http://apl.aip.org/authors>

ADVERTISEMENT



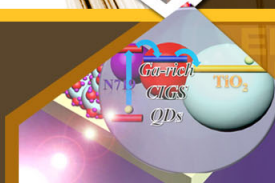
**EXPLORE WHAT'S
NEW IN APL**

SUBMIT YOUR PAPER NOW!



SURFACES AND INTERFACES

Focusing on physical, chemical, biological, structural, optical, magnetic and electrical properties of surfaces and interfaces, and more...



ENERGY CONVERSION AND STORAGE

Focusing on all aspects of static and dynamic energy conversion, energy storage, photovoltaics, solar fuels, batteries, capacitors, thermoelectrics, and more...

Surface plasmon modulation induced by a direct-current electric field into gallium nitride thin film grown on Si(111) substrate

Arnaud Stolz,¹ Suk-Min Ko,² Gilles Patriarche,³ Elhadj Dogheche,^{1,a)} Yong-Hoon Cho,^{2,b)} and Didier Decoster¹

¹*Optoelectronics Department, Institut d'Électronique, Microélectronique et Nanotechnologie, CNRS UMR 8520, Avenue Poincaré, 59 652 Villeneuve d'Ascq, France*

²*Department of Physics and Graduate School of Nanoscience & Technology (WCU), Korea Advanced Institute of Science and Technology (KAIST), Daejeon 305-701, South Korea*

³*Laboratoire de Photonique et Nanostructures, CNRS UPR 20, Route de Nozay, 91 460 Marcoussis, France*

(Received 23 October 2012; accepted 29 December 2012; published online 16 January 2013)

We report here the experimental results on a field effect refractive index change into gallium nitride (GaN) structures. This effect is characterized through the common prism-coupling technique with the application of a vertical direct-current electric field. Surface plasmon propagation was used to increase the sensitivity of the electro-optic measurements. We have obtained a large refractive index variation for GaN epilayer, around 1.4×10^{-2} at $1.55 \mu\text{m}$ wavelength. In order to understand the origin of the index modulation, we have conducted a scanning transmission electron microscopy analysis and discussed the influence of threading dislocations density acting as traps and thermo-optic effect. According to recent works, we observed experimentally the optical response of a non-linear electro-optic effect on GaN on Si(111) substrate and estimated a Kerr coefficient of about $2.14 \times 10^{-16} \text{m}^2 \text{V}^{-2}$. © 2013 American Institute of Physics. [<http://dx.doi.org/10.1063/1.4776671>]

Gallium-nitride (GaN) is a hexagonal-structured III-V wide band gap material that has become a hot topic. Growth techniques are now able to produce good quality thin films through different techniques as metal organic vapor phase epitaxy or magnetron sputtering,¹ that contributes to reducing the defects (grain boundaries, nitrogen vacancies, or unintentionally impurities) which degrade the electronic properties. This is why people have been very interested in GaN optical properties characterization for years. However, conclusions show that linear optical parameters such as the refractive index and propagation losses are as sensitive to these imperfections as electronic ones.² In addition, GaN crystals behave as non-centrosymmetric structures, which indicate they are capable of generating a second-order non-linear optical response. Authors already presented some works on this non-linear characterization in GaN thin films^{3,4} without a real proof of the advantage of all-optic GaN based optoelectronic devices.

We report here the study of electro-optic effect in GaN thin films grown on doped silicon by prism-coupling technique. Scanning transmission electron microscopy (STEM), scanning electron microscopy, and X-ray diffraction (XRD) were conducted for microstructural analysis of the thin film. Prism-coupling was used to measure the optical properties and electro-optic effect. By analyzing the refractive index variation of GaN thin films when applying an orthogonal electric field, we extracted the electro-optic properties of GaN in both light polarization. A comparison with a thermal effect is done to exclude a thermo-optic behavior.

Undoped GaN (u-GaN) was grown on an n-type silicon (111) substrate by metal organic chemical vapor deposition (Sysnex Marvel 260 NT). Prior to growth, the Si(111)

substrates were cleaned in a mixture of H_2SO_4 and deionized water (10:1) at room temperature for 15 min, and rinsed in deionized water. The Si (111) substrates were mounted onto a six-pocket susceptor in the reaction chamber. As a first step, the Si (111) substrates were thermally etched to remove the natural oxide layer at 1120°C in H_2 for 6 min. Trimethyl-gallium, trimethylaluminum, and ammonia (NH_3) were used as alkyl sources for Ga, Al, and N, respectively. An AlN buffer layer (around 40 nm) was grown at 1120°C during 60 min. Then, an $\text{Al}_x\text{Ga}_{1-x}\text{N}$ interlayer was used to reduce the strain due to lattice mismatch between AlN and GaN. $\text{Al}_y\text{Ga}_{1-y}\text{N}/\text{GaN}$ ($x > y$) superlattice was employed to compensate the severe tensile strain during the cooling down due to the thermal expansion coefficient difference and due to the lattice constant mismatch between silicon and GaN. This stack was already studied^{5,6} and consists in 24 periods of $\text{Al}_y\text{Ga}_{1-y}\text{N}/\text{GaN}$ superlattice with a total thickness of around 80 nm.⁷ Finally, $1 \mu\text{m}$ of u-GaN was grown at 1040°C . A schematic of the sample structure is described in Figure 1.

Figure 2 is a bright field (BF) STEM showing the dislocation density within the growth. Figure 2(a) shows that the

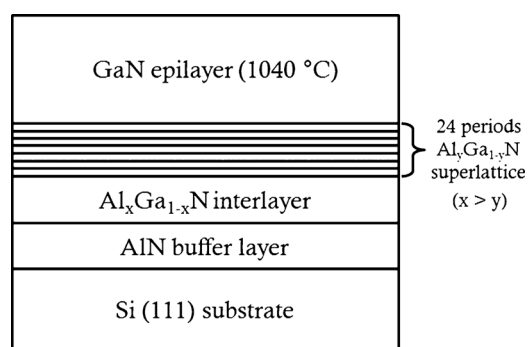


FIG. 1. Schematic representing the sample structure (Al compound: $x > y$).

^{a)}Electronic mail: elhadj.dogheche@univ-valenciennes.fr.

^{b)}Electronic mail: yhc@kaist.ac.kr.

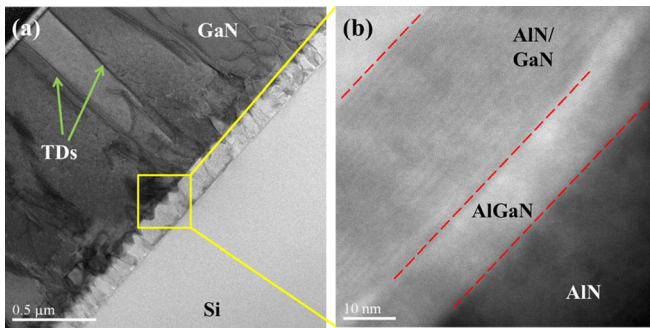


FIG. 2. Analysis of the grown stack on silicon: (a) BF STEM image in large view showing the threading dislocations existing within the top GaN layer (waveguide). (b) Atomic resolution HAADF STEM image of the AlN/GaN superlattices oriented along the $[1\bar{1}00]$ axis.

threading dislocation density is not as high as expected because of the use of very few buffer layers. We estimated the threading dislocations density on the GaN top surface using the value of FWHM of XRD rocking curve^{8,9} from 5 to $8 \times 10^9 \text{cm}^{-2}$. Figure 2(b) is an atomic resolution high angle annular dark field (HAADF) contrast image of the AlN/GaN superlattice oriented along the $[1\bar{1}00]$ axis. The lattice adaptation from AlGaN to GaN is optimized through the AlN/GaN superlattice with well defined short periods. Although the strain compensation layers of the AlGaN/GaN superlattice and the AlGaN interlayer effectively reduced the severe tensile strain applied on the GaN epilayer, the threading dislocation density was slightly increased due to the lattice mismatch at the interfaces of the strain compensation layers.

In order to apply an electric field within the GaN film, a transparent 50 nm-Au top electrode was deposited as Schottky contact by e-beam evaporation after an Ar etching. A Ti(2.5 nm)/Au(100 nm) ohmic contact was deposited by sputtering directly on the doped silicon substrate to form a back electrode. Platinum wires were then pasted to these electrodes using a thermo-conductive resist. The top contact was connected to the common plug and back electrode to the plus of a stabilized voltage generator.

Refractive index measurements were performed using a typical commercial prism-coupler, model M2010 from Metricon. This technique already demonstrated its great accuracy in the linear optical characterization, for refractive indices, elasto-optic coefficients, or propagation losses.¹⁰ We used a GaAs prism to couple light into the GaN layer at a nearly standard telecommunication wavelength of $1.539 \mu\text{m}$. This prism was chosen because of its refractive index that has to be higher than the one of the GaN film. In a previous work, we proved that the threading dislocation density has a direct influence on the refractive index on GaN thin film grown on sapphire substrate through a short-period superlattice buffer layer.¹¹ Similar work was conducted on AlN thin films on silicon.¹²

Figure 3 presents the refractive index variation when a static voltage bias is applied through the GaN thin film. To increase the measure sensitivity, we choose to observe the surface plasmon wave propagating at the Au-GaN interface with a penetration depth of about 500 nm.¹³ Because of the structure geometry, we consider a vertical DC electric field

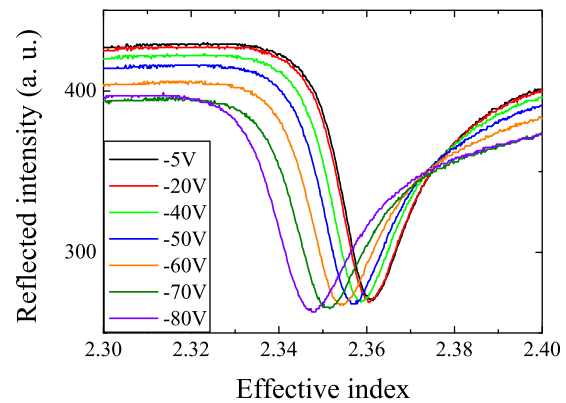


FIG. 3. Surface plasmon effective index variation versus applied voltage. The mode is shifting to lower values when the corresponding electric field is increasing.

perpendicular to the interfaces. After a transitory regime (from 0 to -20V), due to the higher resistivity of the buffer layers, most of the electric field is applied into the top layer because of the electrical conduction of n-doped GaN. In the range of $[-80 \text{V}; -20 \text{V}]$, the surface plasmon wave effective index is shifting from 2.362 up to 2.348, resulting in a negative variation of about 1.4×10^{-2} . Even if the waveguide mode is not as observable as the plasmon ones due to the absorption of silicon, it has a similar variation. The authors already observed such a waveguide refractive index variation on GaN deposited on sapphire¹⁴ but with a lesser order of magnitude. Figure 4(a) shows the index variation as a function of the squared electric field. Because the variation is not proportional to the applied voltage, we cannot consider a linear electro-optic Pockels effect.¹⁵ We also defined a Kerr-like coefficient from the definition $\Delta n = KE^2$, where E is the applied electric field and obtained a value for K of about $2.14 \times 10^{-16} \text{cm}^2 \text{V}^{-2}$, which is in the average of known Kerr coefficients.¹⁶

To exclude a thermal effect, we compared the electric field-induced index variation with the one involved in the heating of the material. A flexible hotplate was fixed on the substrate and a Pt100 thermocouple was applied on the top gold surface. Temperature control was performed with a MINCO setup able to measure index variation in the 298–400 K range.

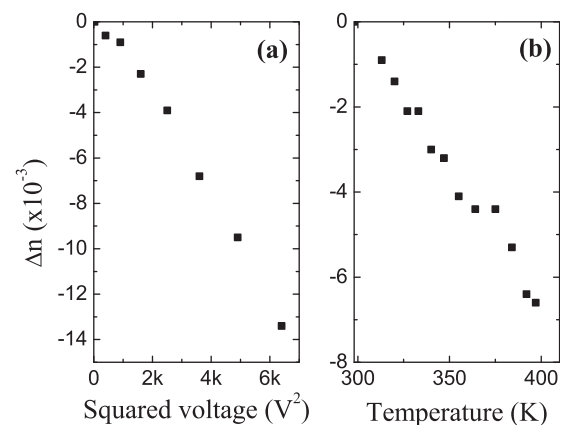


FIG. 4. (a) Surface plasmon effective index variation as a function of the applied electric field on the 2cm^2 surface area. (b) Surface plasmon effective index variation as a function of applied heating to the top total stack (temperature value taken on top of Au-GaN layer).

Figure 4(b) shows the temperature dependent surface plasmon effective index variation. A linear law was used to extract the following coefficient: $\frac{dn}{dT} = -7 \times 10^{-5} \text{K}^{-1}$, which is a common value for a GaN thermo-optic coefficient.¹⁷

To estimate the heating due to the electric field application, we calculated the thermal dissipation within the GaN epilayer. Because of the small difference between GaN¹⁸ ($1.3 \text{ W cm}^{-1} \text{ }^\circ\text{C}^{-1}$) and Si¹⁹ ($1.2 - 1.5 \text{ W cm}^{-1} \text{ }^\circ\text{C}^{-1}$) thermal conductivity, an average value for the total stack was used of $\sigma_{tot} = 1.3 \text{ W cm}^{-1} \text{ }^\circ\text{C}^{-1}$. Associated thermal resistance of the sample is given by

$$R_{th} = \frac{1}{\sigma_{tot}} \frac{e_{tot}}{S_{electrode}} = 0.012 \text{ }^\circ\text{C W}^{-1}, \quad (1)$$

where $e_{tot} = 3 \times 10^{-2}$ is the thickness of the complete stack and $S_{electrode} = 2 \text{ cm}^2$. Considering a maximum electrical power of 10 W (corresponding to 5 W cm^{-2} on 2 cm^2), the temperature increase on the electrode is about $0.12 \text{ }^\circ\text{C}$. As a correlation, no heating was observed under infra-red thermal camera while applying voltage.

In summary, we exhibit a high non-linear field effect refractive-index variation on GaN thin film grown on doped silicon. Neither the threading dislocations density nor the thermo-optic behavior in GaN explains the electrically induced index variation in GaN. We conclude that this poorly known effect is related to both inverse electrostriction effect and elasto-optic effect. Compressive stress is electrically induced through a second-order electrostriction process²⁰ and reduces the lattice parameter in the orthogonal direction to the surface. As a consequence, refractive indices decrease proportionally under a linear elasto-optic behavior.^{10,21} In these terms, we concluded to a non-linear Kerr-like electro-optic effect, proportional to the squared applied voltage, which is optically confirmed.

The authors are grateful to Eric Vivien from French Embassy in South Korea for making this collaboration possible through an EGIDE project structure. The work at KAIST was supported by the WCU Program (No. R31-2008-000-

10071-0) of the Ministry of Education, Science and Technology. The authors are grateful to Rose-Marie Sauvage from DGA and to Aurélien Gauthier-Brun from IEMN too.

¹X. Zhang, B. Soderman, E. Armour, and A. Paranjpe, *J. Cryst. Growth* **318**, 436–440 (2011).

²S.-E. Park, W. Han, H. Lee, and B. O. J. *Crystal Growth* **253**, 107–111 (2003).

³J. Miragliotta, D. K. Wickenden, T. J. Kistenmacher, and W. A. Bryden, *J. Opt. Soc. Am. B* **10**, 1447–1456 (1993).

⁴H. Jiang and J. Singh, *Appl. Phys. Lett.* **75**, 1932–1934 (1999).

⁵S.-H. Jang and C.-R. Lee, *J. Cryst. Growth* **253**, 64–70 (2003).

⁶C. Huang, S. Chang, R. Chuang, J. Lin, Y. Cheng, and W. Lin, *Appl. Surf. Sci.* **256**, 6367–6370 (2010).

⁷M. Wei, X. Wang, X. Pan, H. Xiao, C. Wang, Q. Hou, and Z. Wang, *Mater. Sci. Semicond. Process.* **14**(2), 97–100 (2011).

⁸V. M. Kaganer, O. Brandt, A. Trampert, and K. H. Ploog, *Phys. Rev. B* **72**, 045423–045434 (2005).

⁹A. Vilalta-Clemente, G. R. Mutta, M.-P. Chauvat, M. Morales, J.-L. Doualan, P. Ruterana, M. A. Sanchez-Garcia, F. Calle, E. Valcheva, and K. Kirilov, *Phys. Status Solidi A* **207**(5), 1079–1082 (2010).

¹⁰S. Pezzagna, J. Brault, M. Leroux, J. Massies, and M. de Micheli, *J. Appl. Phys.* **103**, 123112 (2008).

¹¹A. Stolz, E. Cho, E. Dogheche, Y. Androussi, D. Troadec, D. Pavlidis, and D. Decoster, *Appl. Phys. Lett.* **98**, 161903 (2011).

¹²F. Natali, F. Semon, J. Massies, D. Byrne, S. Laugt, O. Tottreau, P. Vennegues, E. Dogheche, and E. Dumont, *Appl. Phys. Lett.* **82**, 1386–1388 (2003).

¹³A. Stolz, L. Considine, S. Faci, E. Dogheche, C. Tripon-Canseliet, B. Loiseaux, D. Pavlidis, D. Decoster, and J. Chazelas, *Opt. Lett.* **37**, 3039–3041 (2012).

¹⁴A. Stolz, L. Considine, E. Dogheche, D. Decoster, and D. Pavlidis, *IEICE Trans. Electron.* **E95-C**(8), 1363–1368 (2012).

¹⁵X.-C. Long, R. A. Myers, S. R. J. Brueck, R. Ramer, K. Zheng, and S. D. Hersee, *Appl. Phys. Lett.* **67**(10), 1349–1351 (1995).

¹⁶R. L. Sutherland, *Handbook of Nonlinear Optics* (Marcel Dekker, Inc., New York, 2003), pp. 866–868.

¹⁷N. Watanabe, T. Kimoto, and J. Suda, *Proc. SPIE* **7926**, 792604 (2011).

¹⁸T. P. Chow and M. Ghezzi, in III-Nitride, SiC, and Diamond Materials for Electronic Devices Material Research Society Symposium Proceedings (1996), pp. 69–73.

¹⁹C. J. Glassbrenner and G. A. Slack, *Phys. Rev.* **134**(4A), A1058–A1069 (1964).

²⁰L. Pedesseau, C. Katan, and J. Even, *Appl. Phys. Lett.* **100**, 031903 (2012).

²¹M. Fukuzawa, R. Kashiwagi, and M. Tamada, *Phys. Status Solidi C* **8**(2), 432–434 (2011).